

Simultaneous wavelength conversion of ASK and DPSK signals based on four-wave-mixing in dispersion engineered silicon waveguides

Lin Xu,^{1,*} Noam Ophir,¹ Michael Menard,² Ryan Kin Wah Lau,³ Amy C. Turner-Foster,² Mark A. Foster,³ Michal Lipson,^{2,4} Alexander L. Gaeta,³ and Keren Bergman¹

¹Department of Electrical Engineering, Columbia University, New York, NY 10027, USA

²School of Electrical and Computer Engineering, Cornell University, Ithaca, NY 14853, USA

³School of Applied and Engineering Physics, Cornell University, Ithaca, NY 14853, USA

⁴Kavli Institute at Cornell for Nanoscale Science, Cornell University, Ithaca, NY 14853, USA

*lx2140@columbia.edu

Abstract: We experimentally demonstrate four-wave-mixing (FWM)-based continuous wavelength conversion of optical differential-phase-shift-keyed (DPSK) signals with large wavelength conversion ranges as well as simultaneous wavelength conversion of dual-wavelength channels with mixed modulation formats in 1.1-cm-long dispersion-engineered silicon waveguides. We first validate up to 100-nm wavelength conversion range for 10-Gb/s DPSK signals, showcasing the capability to perform phase-preserving operations at high bit rates in chip-scale devices over wide conversion ranges. We further validate the wavelength conversion of dual-wavelength channels modulated with 10-Gb/s packetized phase-shift-keyed (PSK) and amplitude-shift-keyed (ASK) signals; demonstrate simultaneous operation on multiple channels with mixed formats in chip-scale devices. For both configurations, we measure the spectral and temporal responses and evaluate the performances using bit-error-rate (BER) measurements.

©2011 Optical Society of America

OCIS codes: (130.7405) Wavelength conversion devices; (190.4380) Nonlinear optics, four-wave mixing; (190.4390) Nonlinear optics, integrated optics; (060.5060) Phase modulation.

References and links

1. Q. Lin, J. Zhang, P. M. Fauchet, and G. P. Agrawal, "Ultrabroadband parametric generation and wavelength conversion in silicon waveguides," *Opt. Express* **14**(11), 4786–4799 (2006).
2. B. G. Lee, A. Biberman, A. C. Turner-Foster, M. A. Foster, M. Lipson, A. L. Gaeta, and K. Bergman, "Demonstration of broadband wavelength conversion at 40 Gb/s in silicon waveguides," *IEEE Photon. Technol. Lett.* **21**(3), 182–184 (2009).
3. N. Ophir, J. Chan, K. Padmaraju, A. Biberman, A. C. Foster, M. A. Foster, M. Lipson, A. L. Gaeta, and K. Bergman, "Continuous wavelength conversion of 40-Gb/s Data Over 100 nm using a dispersion-engineered silicon waveguide," *IEEE Photon. Technol. Lett.* **23**(2), 73–75 (2011).
4. L. Xu, N. Ophir, E. Swan, A. C. Turner-Foster, M. A. Foster, M. Lipson, A. L. Gaeta, and K. Bergman, "Broadband wavelength conversion of 10-Gb/s DPSK signals in silicon waveguides," *Photonics Society Annual Meeting, Denver, TuT3* (2010).
5. H. Hu, E. Palushani, M. Galili, H. C. H. Mulvad, A. Clausen, L. K. Oxenløwe, and P. Jeppesen, "640 Gbit/s and 1.28 Tbit/s polarisation insensitive all optical wavelength conversion," *Opt. Express* **18**(10), 9961–9966 (2010).
6. H. Hu, H. Ji, M. Galili, M. Pu, H. C. H. Mulvad, L. K. Oxenløwe, K. Yvind, J. M. Hvam, and P. Jeppesen, "Silicon chip based wavelength conversion of ultra-high repetition rate data signals", *Optical Fiber Communication Conference, Los Angeles, postdeadline paper, PDP A8* (2011).
7. T. V. Andersen, K. M. Hilligsøe, C. K. Nielsen, J. Thøgersen, K. Hansen, S. Keiding, and J. Larsen, "Continuous-wave wavelength conversion in a photonic crystal fiber with two zero-dispersion wavelengths," *Opt. Express* **12**(17), 4113–4122 (2004).
8. C. M. Gallep, H. J. S. Dorren, and O. Raz, "Four-wave-mixing-based dual-wavelength conversion in a semiconductor optical amplifier," *IEEE Photon. Technol. Lett.* **22**(21), 1550–1552 (2010).

9. J. Yamawaku, A. Takada, E. Yamazaki, O. Tadanaga, H. Miyazawa, and M. Asobe, "Selective wavelength conversion using PPLN waveguide with two pump configuration," in Conf. Lasers and Electro-Optics, Baltimore, CWB5(2003).
10. M. D. Pelusi, F. Luan, S. Madden, D.-Y. Choi, D. A. Bulla, B. Luther-Davies, and B. J. Eggleton, "Wavelength conversion of high-speed phase and intensity modulated signals using a highly nonlinear chalcogenide glass chip," *IEEE Photon. Technol. Lett.* **22**(1), 3–5 (2010).
11. A. O. J. Wiberg, C. S. Bres, B. P. P. Kuo, J. M. C. Boggio, N. Alic, and S. Radic, "Multicast parametric synchronous sampling of 320-Gb/s return-to-zero signal," *IEEE Photon. Technol. Lett.* **21**(21), 1612–1614 (2009).
12. A. Biberman, B. G. Lee, A. C. Turner-Foster, M. A. Foster, M. Lipson, A. L. Gaeta, and K. Bergman, "Wavelength multicasting in silicon photonic nanowires," *Opt. Express* **18**(17), 18047–18055 (2010).
13. Y. Dai, X. Chen, Y. Okawachi, A. C. Turner-Foster, M. A. Foster, M. Lipson, A. L. Gaeta, and C. Xu, "1 microsecond tunable delay using parametric mixing and optical phase conjugation in Si waveguides," *Opt. Express* **17**(9), 7004–7010 (2009).
14. R. Salem, M. A. Foster, A. C. Turner, D. F. Geraghty, M. Lipson, and A. L. Gaeta, "Signal regeneration using low-power four-wave mixing on silicon chip," *Nat. Photonics* **2**(1), 35–38 (2008).
15. M. A. Foster, A. C. Turner, J. E. Sharping, B. S. Schmidt, M. Lipson, and A. L. Gaeta, "Broad-band optical parametric gain on a silicon photonic chip," *Nature* **441**(7096), 960–963 (2006).
16. T. D. Vo, H. Hu, M. Galili, E. Palushani, J. Xu, L. K. Oxenlowe, S. J. Madden, D.-Y. Choi, D. A. P. Bulla, M. D. Pelusi, J. Schroder, B. Luther-Davies, and B. J. Eggleton, "Photonic chip based transmitter optimization and receiver demultiplexing of a 1.28 Tbit/s OTDM signal," *Opt. Express* **18**(16), 17252–17261 (2010).
17. H. Ji, M. Galili, H. Hu, M. Pu, L. K. Oxenlowe, K. Yvind, J. M. Hvam, and P. Jeppesen, "1.28 Tb/s demultiplexing of an OTDM DPSK data signal using a silicon waveguide," *IEEE Photon. Technol. Lett.* **22**(23), 1762–1764 (2010).
18. A. C. Turner, C. Manolatu, B. S. Schmidt, M. Lipson, M. A. Foster, J. E. Sharping, and A. L. Gaeta, "Tailored anomalous group-velocity dispersion in silicon channel waveguides," *Opt. Express* **14**(10), 4357–4362 (2006).
19. A. C. Turner-Foster, M. A. Foster, R. Salem, A. L. Gaeta, and M. Lipson, "Frequency conversion over two-thirds of an octave in silicon nanowaveguides," *Opt. Express* **18**(3), 1904–1908 (2010).
20. E. Dulkeith, Y. A. Vlasov, X. Chen, N. C. Panoiu, and R. M. Osgood, Jr., "Self-phase-modulation in submicron silicon-on-insulator photonic wires," *Opt. Express* **14**(12), 5524–5534 (2006).

1. Introduction

As data rates in broadband optical networks continues to grow, all-optical signal processing technologies are expected to become essential for energy efficient optical switch fabrics since signal manipulation based on optical-electrical-optical (OEO) interfaces will become too complex and power hungry at high multichannel data rates. Optical parametric processing platforms enable power efficient and ultra-fast signal processing functionalities for wavelength converters [1–10], wavelength multicasters [11,12], tunable delays [13], regenerators [14], amplifiers [15], as well as temporal demultiplexers [16,17]. Among these functionalities, wavelength converters are critical building blocks for wavelength-division-multiplexed (WDM) systems as they can help avoid wavelength contention problems and increase overall system flexibility. Ideally in such a system, it is required to be format transparent, i.e., mixed-format channels can be wavelength converted in a single device over a wide wavelength range. Parametric wavelength converters based on four-wave-mixing (FWM) have been demonstrated in highly-nonlinear fiber (HNLF) [6], photonic crystal fiber (PCF) [7], semiconductor optical amplifier (SOA) [8], periodically poled LiNbO₃ (PPLN) [9], chalcogenide waveguides [10], as well as silicon waveguides [1–5]. However, these demonstrations cannot fully satisfy the aforementioned requirements.

Complementary metal-oxide-semiconductor (CMOS)-compatible silicon photonic devices are attractive for all optical processing systems since they possess potential for low-cost mass production, and are typically of very small-footprint allowing for dense integration of these devices. Moreover, the silicon waveguides' well-controlled sub-micron cross-section dimensions allow for tight control of modal dispersion properties, allowing for dispersion engineering to optimize four-wave mixing (FWM) bandwidth and efficiency [1,18]. Thus far, terabit-per-second bit rates processing within the telecom bands [16,17] and up to 800-nm continuous wavelength conversion bandwidth with continuous wave (CW) signal [19] have been experimentally demonstrated, showing the potential for ultra-broadband and ultra-high

bit rate parametric processing systems based on silicon photonic technology. Phase-shift-keyed (PSK) format is widely used in today's optical communication systems as it exhibits several advantageous qualities such as improved receiver sensitivity, higher tolerance to effects of nonlinear degradation, and potential for improved spectral efficiency. Previous demonstrations of wavelength conversion in silicon waveguides have focused on amplitude-shift-keyed (ASK) format [2-3,12]. The capacity of these silicon waveguides to achieve broadband wavelength conversion of PSK format and simultaneous wavelength conversion of dual-channel with mixed formats (one modulated in PSK format while the other in ASK format) have yet to be explored.

In this paper, we report two recent demonstrations. In the first, we wavelength convert a 10-Gb/s DPSK signal in a dispersion engineered silicon waveguide across 100-nm wavelength range, thus validating the capacity of these silicon waveguides for ultra-broadband and format transparent parametric processing. The DPSK probe signal is repeatedly wavelength converted using a strong CW pump with varied probe-idler separations, and the performance of this functionality is evaluated by measuring the bit-error-rate (BER) curves. Error-free operations with a constant 1-dB power penalty over a range of probe-idler separations spanning 100-nm wavelength range are achieved. In the second demonstration we experimentally demonstrate simultaneous wavelength conversion of dual-wavelength channels with mixed formats in a dispersion engineered silicon waveguide, further validating the capacity of these silicon waveguides for parametric processing of different formats simultaneously. One-channel and two-channel wavelength conversions of 10-Gb/s packetized data (ASK + PSK) using strong gated CW pumps are achieved with error-free operation and less than 0.4-dB power-penalty difference between the two configurations.

2. Broadband wavelength conversion

Since both ASK and PSK formats are widely used in optical networks, future wavelength converters should be format transparent with the ability to use the exact same component to wavelength convert any incoming data format. As FWM-based wavelength conversion is a phase-preserving operation, we expect phase modulated data to be wavelength converted with minimal degradation. In order to verify the suitability of the silicon waveguides for this functionality in a broadband manner, we wavelength-convert a 10-Gb/s DPSK signal with varied conversion ranges to show consistent low power penalties for the different conversion ranges.

2.1 Experimental setup

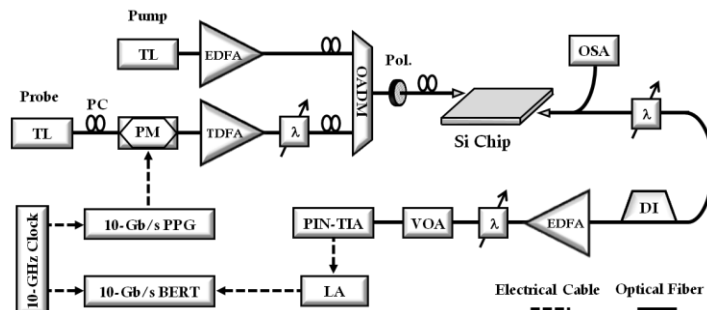


Fig. 1. Experimental setup for broadband wavelength conversion of 10-Gb/s DPSK signals.

The experimental setup for this demonstration is schematically shown in Fig. 1. A CW probe from a tunable laser (TL) is modulated by a phase modulator, driven with a 10-Gb/s non-return-to-zero (NRZ) $2^{31}-1$ pseudo-random bit sequence (PRBS) data from a pulse pattern generator (PPG), to generate a DPSK signal. The modulated probe signal is then amplified by a thulium-doped amplifier (TDFA) and filtered (λ) using a tunable filter. A CW pump signal

at 1552.5 nm from another TL is amplified using an erbium-doped fiber amplifier (EDFA) and combined with the probe using an optical add-drop multiplexer (OADM). Polarization controllers are used throughout the experiment for polarization optimization. Both the probe and pump signals are aligned to TE polarization with a total power of 22 dBm before being injected onto the chip using a tapered fiber. The device used here is a silicon waveguide of 1.1-cm length, 30-nm slab and 290-nm × 720-nm cross section with fiber-to-fiber linear insertion loss of ~6.4 dB, fabricated at Cornell Nanofabrication Facility using electron-beam lithography followed by reactive-ion etching. Each end of the waveguide has an inverse-taper mode converter for efficient coupling to tapered fibers. The zero-group-velocity-dispersion (ZGVD) wavelength for this waveguide was calculated to be ~1577 nm [19]. The optical signal egressing from the chip is measured with an optical spectrum analyzer (OSA). The converted signal is filtered and demodulated using a delay interferometer (DI) before undergoing additional amplification and filtering. The demodulated signal is inspected using a digital communications analyzer (DCA), received using a photodetector (PIN-TIA) followed by a limiting amplifier (LA), and measured with a BER tester (BERT). A variable optical attenuator (VOA) is used to vary the optical power incident on the receiver for the BER measurements. Back-to-back eye diagrams and the corresponding BER curves are recorded bypassing the chip, and then detected with no amplifier afterwards.

2.2 Experimental results

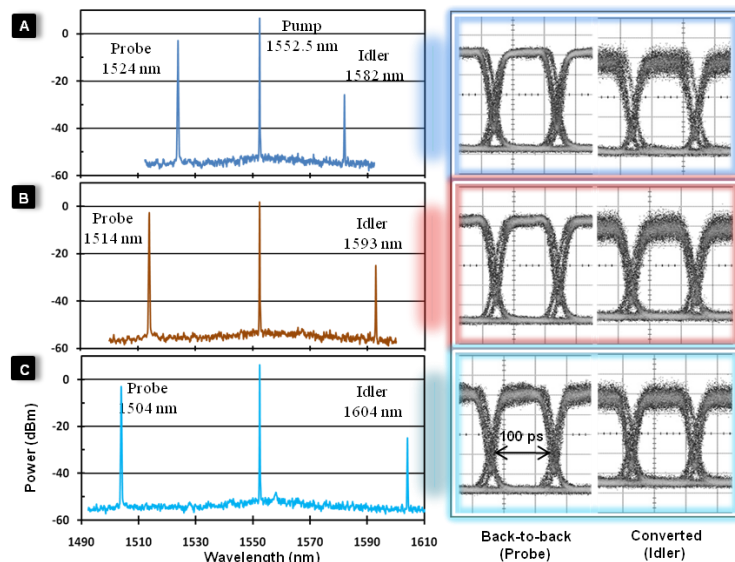


Fig. 2. Spectra after FWM (left) and respective eye diagrams (right) of back-to-back and converted cases for broadband wavelength conversion of 10-Gb/s DPSK signals, corresponding to conversion range of (a) 58 nm (b) 79 nm (c) 100 nm

In order to observe the device's operation with large probe-idler detuning, we perform several wavelength conversions with separate probe wavelengths set to 1524, 1514, and 1504 nm, corresponding to probe-idler detunings of 58, 79, and a 100 nm respectively. We measure the spectra of the wavelength conversions directly after the chip and the corresponding eye diagrams for the probe and idler as shown in Fig. 2a-c. The conversion efficiency (the difference in power between the probe and idler egressing from the chip) remains constant -24 dB, and the converted eye diagrams remain clean and open with different conversion ranges. We then measure bit-error-rate (BER) for both back-to-back (probe) and converted (idler) signals as shown in Fig. 3. The BER curves of the converted signals overlap and a constant minimal power penalty of 1 dB as well as error-free operation are experimentally

achieved for all the wavelength conversion ranges. The power penalty mainly comes from the amplified spontaneous emission (ASE) noise from the preamplifier, filtering stage.

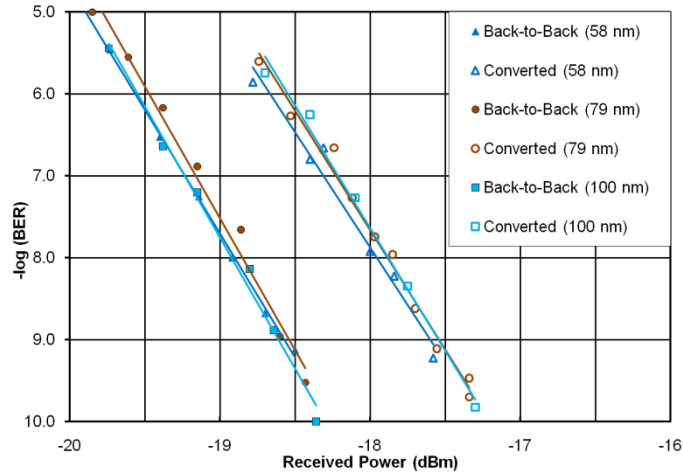


Fig. 3. 10-Gb/s BER curves of back-to-back and wavelength-converted signals with constant 1-dB power penalties for probe-idler separations of 58, 79, and 100 nm respectively.

3. Mixed-format wavelength conversion

Beyond being able to wavelength-convert both ASK and PSK data, it would be beneficial to be able to simultaneously process more than one signal channel with different formats to reduce complexity and cost on the system level. Therefore we proceed to demonstrate a higher complexity functionality with packetized dual-wavelength conversion of mixed-format signals, enabling simultaneous operation with different modulation formats and multi-channels at high bit rates in chip-scale devices to affirm the feasibility of simultaneous conversion of multiple channels with different formats. Data measurements are performed to validate the feasibility of this functionality.

3.1 Experimental setup

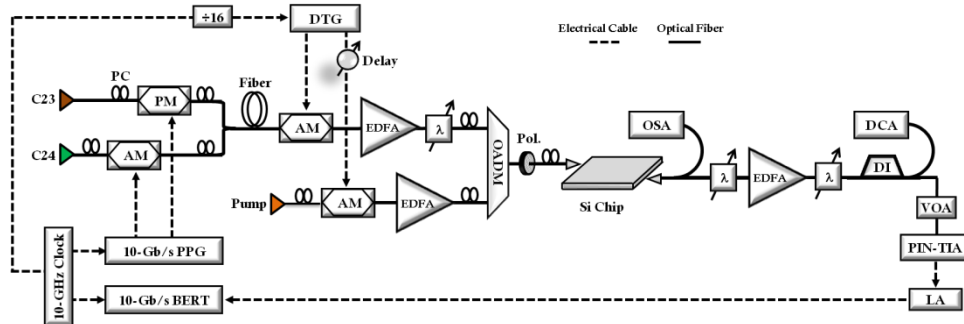


Fig. 4. Experimental setup for mixed formats (ASK + PSK) wavelength conversion

The experimental setup for this demonstration is schematically shown in Fig. 4. Two CW probe signals at 1559 nm and 1558.1 nm (occupying the wavelength channel of C23 and C24 within ITU grid) from distributed feedback (DFB) lasers are modulated by a phase modulator and an amplitude modulator respectively, both driven by 10-Gb/s data (NRZ, 2^{15} -1 PRBS) from a PPG, to generate optical PSK and ASK signals. They are then combined using a 3-dB coupler and sent to 6.5-km single mode fiber for data decorrelation. After that, they are gated using another amplitude modulator driven by a data timing generator (DTG) which outputs

192-ns period with 25% duty cycle, producing 48-ns optical packets. Using gated pump and probes also enhances the conversion efficiency by increasing the peak power while maintaining the average power low, minimizing two-photon absorption (TPA) and TPA-induced free-carrier absorption (FCA) losses. The packetized probe signals are further amplified and filtered using an EDFA and a broadband tunable filter. In parallel, a CW pump signal at 1552.5 nm (C31, ITU grid) from a TL is also gated using an amplitude modulator driven with the same DTG output which is electronically delayed to ensure the packets of the pump and the probe signals overlap in time domain perfectly. The pump signal is then amplified and combined with the probe signals using an OADM. All the signals are aligned to TE polarization before being launched into the silicon chip with a tapered fiber.

The device used here is similar to the one described previously but fabricated in a different run. It has a 300-nm × 710-nm cross section, 1-cm length and fiber-to-fiber linear insertion loss of ~8.8 dB. Dispersion profile characterization has been reported previously for these designs and was not measured within this experiment. The FWM interaction in the silicon waveguide produces idlers at shorter wavelengths which are copies of the probes. The optical signals egressing from the chip are coupled out via another tapered fiber and examined on an OSA first. Then the converted signal is filtered using a tunable grating filter, amplified using an EDFA and further filtered using a second tunable grating filter to suppress ASE noise. The converted PSK signal is demodulated using a DI. The ASK and demodulated PSK signals are then measured using a DCA, received using a PIN-TIA followed by a LA, and finally measured on a BERT. A common 10-GHz clock is used to synchronize the PPG, DTG, DCA and BERT. The BERT is synchronized with the packet gating signal to ensure that the data portion of the packet is measured without the intensity overshoot at the beginning of each packet. A VOA is used to vary the optical power incident on the receiver for BER measurements. In order to investigate the power penalty from the FWM process only, back-to-back BER curves and the corresponding eye diagrams are recorded bypassing the chip, attenuated using a VOA to mimic the same fiber-to-fiber insertion loss through the chip for each case, and then detected using the same setup.

3.2 Experimental results

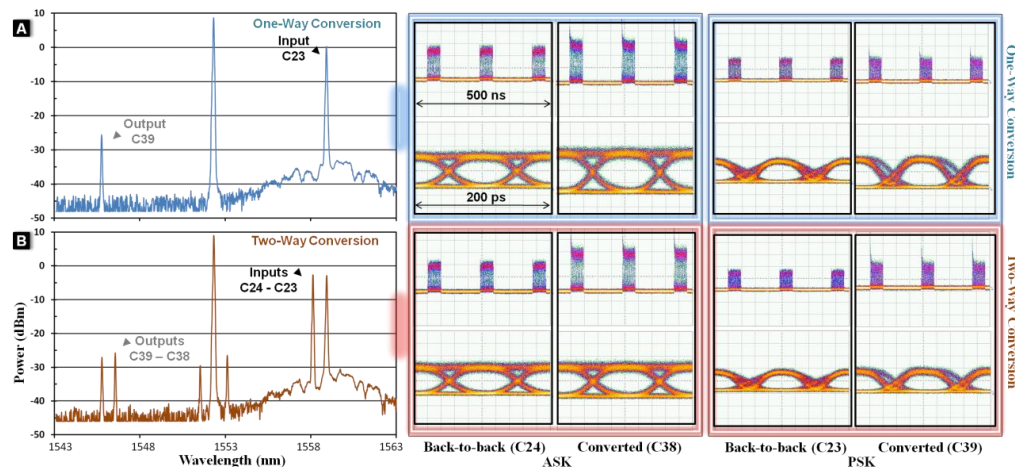


Fig. 5. Recorded spectra (left) and the corresponding time domain responses (right) for mixed-format wavelength conversion (10-Gb/s PSK + 10-Gb/s ASK). (a) One-channel wavelength conversion with single format at each time (b) two-channel wavelength conversion with mixed format. The time windows are 500 ns for packets and 200 ps for the corresponding eye-diagram.

We first perform one-channel wavelength conversion for each channel individually. The optical PSK (ASK) channel at C23 (C24) of ITU grid is converted to shorter wavelength

channel at C39 (C38) through FWM process in the silicon waveguide. After that, we perform two-channel wavelength conversions of mixed-format data by turning on both the PSK (C23) and ASK (C24) channels. Channels at C23 and C24 are simultaneously wavelength converted to C38 and C39. In the experiment, the total average power before entering the chip is kept at 22 dBm for all the cases. We record the optical spectra as well as time domain responses for the optical packets, the corresponding eye diagrams at the output of the chip for the above two configurations as shown in Fig. 5a-b. The conversion efficiencies for both one-channel and two-channel conversion configurations are -25 dB. The overshoot at the beginning of each converted packet is due to TPA and FCA as a result of the “packetized” pump. This can be avoided by using slightly longer pump which starts earlier than the packetized data. The optical packets and respective eye diagrams of both PSK and ASK channels remain clean and open after wavelength conversion with different configurations.

We then record BER curves (Fig. 6) for all the back-to-back (probe) and wavelength-converted (idler) signals for aforementioned cases with error-free operations. The power penalty between the wavelength converted ASK signal and the corresponding back-to-back case is 0.9 dB for one-channel conversion configuration (Fig. 6a), and 1.2 dB for two-channel conversion configuration (Fig. 6b). The power penalty between the wavelength converted PSK signal and the corresponding back-to-back case is 0.4 dB for one-channel conversion configuration (Fig. 6c), and 0.8 dB for two-channel conversion configuration (Fig. 6d). The peak power of the probe signal is above the threshold of nonlinear effects, such as self-phase modulation which accounts for the increased power penalty for ASK one-channel conversion and cross-phase modulation which accounts for the increased power penalty for two-channel conversion [20].

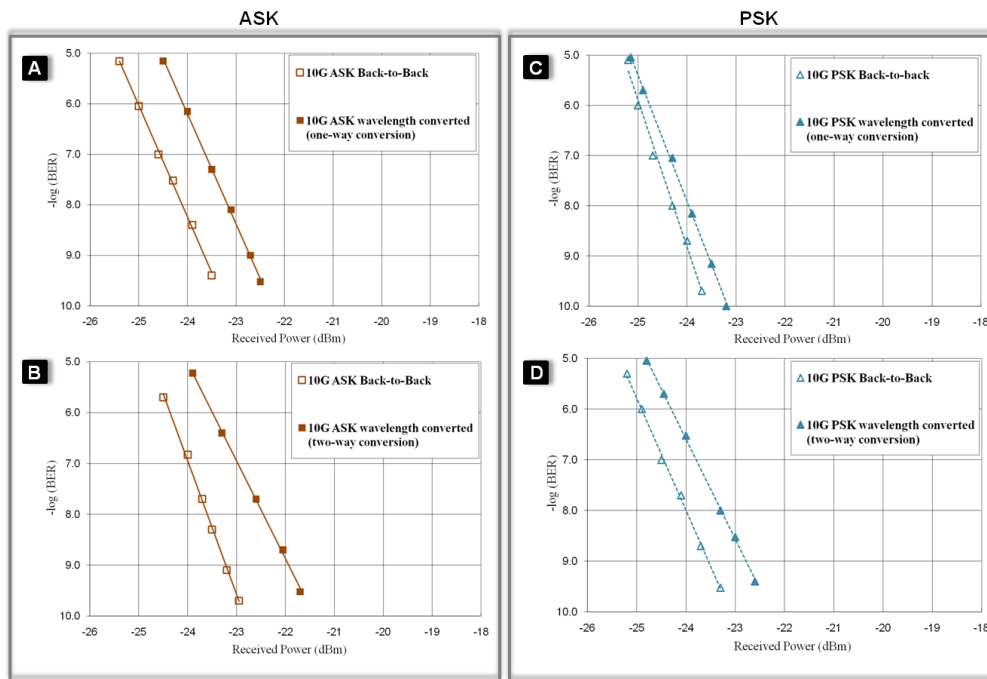


Fig. 6. BER curves measured for all the back-to-back cases (probes) and wavelength-converted cases (idlers). (a) one-channel conversion and (b) two-channel conversion for ASK signals. (c) one-channel conversion and (d) two-channel conversion for PSK signals.

4. Conclusion

We have validated the silicon-photonics platform's suitability for FWM-based wavelength conversion of phase modulated signals over a broad spectrum as well as the ability to simultaneously convert multiple channels with mixed formats. In the first demonstration we demonstrated the concept of broadband wavelength conversion of 10-Gb/s DPSK signal over 100 nm utilizing the phase-preserving properties of the all-optical interaction. We observed constant 1-dB power penalty after wavelength conversion for all the examined probe-idler separations. The results affirm the feasibility of format-transparent continuous wavelength converters operating over 100-nm probe-idler detuning using silicon-based FWM devices. We then continued to demonstrate packetized dual-wavelength conversion of mixed-format signals, enabling simultaneous operation with different modulation formats and multi-channels at high bit rates in chip-scale devices. The increased power penalty when scaling to two channels is mainly attributed to the cross phase modulation between the probe signals. Improved performance can be obtained by further optimizing power levels of the probe signals which would allow minimizing deleterious nonlinear cross-talk and still maintaining good optical signal-to-noise ratio (OSNR) of the converted signals. These demonstrations validate the suitability of the CMOS-compatible silicon-photonics platform for flexible low-cost all-optical processing systems and highlight the ability to process multiple data formats on a single platform.

Acknowledgements

This work was supported by the DARPA MTO Parametric Optical Processes and Systems Program under Contract W911NF-08-1-0058 and NSF through CIAN ERC under grant #EEC-0812072. This work was performed in part at the Cornell Nanoscale Facility, a member of the National Nanotechnology Infrastructure Network, which is supported by the NSF.